International Journal of Mechanical Engineering and Applications
2022; 10(4): 68-81
http://www.sciencepublishinggroup.com/j/ijmea
doi: 10.11648/j.ijmea.20221004.14
ISSN: 2330-023X (Print); ISSN: 2330-0248 (Online)

The Development of a Precise Articulated Bus Prediction Model for Model Predictive Control Algorithms

Beomjoon Pyun[1, 2], Jaehoon Jeon[2], Jaemin Song[2], Hyungjeen Choi[2, *]

[1]School of Electrical Engineering, Korea Advanced Institute of Science & Technology, Daejeon, Republic of Korea

[2]Korea Automotive Technology Institute, Cheonan City, Republic of Korea

Email address:

bjpyun@katech.re.kr (Beomjoon Pyun), jhjeon@katech.re.kr (Jaehoon Jeon), jmsong@katech.re.kr (Jaemin Song), jchoi@katech.re.kr (Hyungjeen Choi)

[*]Corresponding author

To cite this article:

Beomjoon Pyun, Jaehoon Jeon, Jaemin Song, Hyungjeen Choi. The Development of a Precise Articulated Bus Prediction Model for Model Predictive Control Algorithms. *International Journal of Mechanical Engineering and Applications*. Vol. 10, No. 4, 2022, pp. 68-81.
doi: 10.11648/j.ijmea.20221004.14

Received: July 31, 2022; **Accepted**: August 23, 2022; **Published**: August 31, 2022

Abstract: This study presents a precise prediction model that can be applied to model-based control logic for the realization of autonomous driving systems (ADS) for bus rapid transit (BRT; articulated buses). When realizing model-based control logic, the more a prediction model is accurate, the greater that control logic will be the robustness. However, a heavy prediction model is not recommended for real-time operation of model based control logic. Therefore, in this study, a revised 'Multi-axle dynamics model' is used to develop a prediction model which is considering dominant parts of longitudinal, lateral, and roll dynamics. Consequently, this study shows the process of testing BRT buses (the targets), and designing a prediction model by comparing with the test results. As a result, a BRT prediction model is developed with correlation of 92% or above. Furthermore, the prediction model will be applied in the future to a model predictive control (MPC) algorithm and used to construct ADS for BRT buses. In addition, it is anticipated that the use of this prediction model will contribute to the design of control logic for diverse advanced driver assistance systems (ADAS).

Keywords: Autonomous Driving Systems (ADS), Articulated Bus, Bus Rapid Transit (BRT), Inner Model, Model Predictive Control (MPC), Modeling, Prediction Model, Vehicle Test

1. Introduction

In recent years, the development of autonomous driving systems (ADS) has been a major issue in the automotive industry. In terms of the hardware, ADS can be divided largely into the sensor, the controller, and the actuator. Out of them, the controller is important in being akin to the brain controlling the vehicle's movements from sensed information of surroundings. Much research and development (R & D) continues to be conducted on ADS controllers even now. As a trend toward autonomous driving control algorithms in recent years, control algorithm design methods using vehicle models have risen in reliability. Therefore, the contents of the control methods will be explained first.

Autonomous driving control algorithms using vehicle models have been studied in diverse ways. The first one is the pure pursuit method [1-3]. Developed in 1988 to control a vehicle named TerraGator, this adopted the method of controlling the vehicle through the use of a bicycle model [4], with the rear-axle center as the standard. Though the control was smooth, it had the disadvantage of being unable to avoid obstacles. The second one is the Stanley method [5-7]. Consisting of control algorithms that enabled Stanford University to win in the 2005 DARPA Grand Challenge, this adopted the method of controlling the vehicle through the use of a bicycle model, with the front-axle center as the standard. Though it makes possible the steady tracking of the path, this method has the disadvantage of control that is not smooth, thus making passengers uncomfortable. A recent autonomous driving control method is the model predictive control (MPC) method [8-10]. Developed in 1980 for processes at chemical plants, it began to be used as autonomous driving control algorithms in 2001. Because the MPC method employs optimized control inputs derived by using the vehicle's

dynamics model, they can be a better algorithm in consideration of the ride quality and tracking.

This study suggests a precise prediction model to use in the MPC algorithm. Specifically, this study presents contents related to the development of a prediction model for bus rapid transit (BRT; articulated buses). And, the BRT buses has several unusual properties to develop the control algorithm. First, the BRT buses are operated in the Cheongna area of Incheon-city, where BRT-only lanes exist and the buses run repeatedly. In addition, because BRT buses are electric vehicles with battery packs mounted on the roofs, they have been designed in consideration of rollover robustness, passengers' ride quality, and urban operation. Consequently, these BRT buses are equipped with acceleration and deceleration limit algorithms. In conclusion, because the properties serve to reduce unpredicted contingencies, the ADS for BRT buses is highly feasible. This study gives a first step to develop a precise prediction model for the MPC algorithm of BRT buses. The prediction model is studied in many ways [11-13]. In this study, 'Multi-axle dynamics model [11]' is mainly considered because of real-time feasibility and roll state.

The introduction to the development of the BRT prediction model is structured as follows. Chapter 2.1 presents contents of a BRT bus tests. Because reference data to be compared with a prediction model are necessary, preparation and test of the vehicle are introduced first. Chapter 2.2 presents a theoretical approach to the prediction model that employs equations. The equations are derived from a reference paper [11], and revised for a BRT bus prediction model. Chapter 2.3 explains a realization of the prediction model. It explains the realization through MATLAB/Simulink and parameters, which are applied in the model. Chapter 3.1 presents the results of the verification of the prediction model. For the verification, three representative scenarios are chosen and verified using correlation equations [14]. Chapter 3.2 introduces a revised prediction model for the construction of MPC algorithms. In this chapter, prediction model equations are combined into matrices in the Ax + Bu form for MPC algorithms. In conclusion, this study has designed a precise prediction model, and the prediction model will be used to design MPC autonomous driving algorithms.

2. The Development of a BRT Prediction Model

2.1. Vehicle Tests of a BRT Bus

To design a prediction model, vehicle tests must be conducted first to serve as a reference. In this study, a target vehicle (BRT bus) is prepared with additional devices and tested according to the scenarios.

Figure 1. *Test devices for the preparation of vehicle tests and the locations.*

As for the construction of an environment for vehicle tests, additional mounting devices that make it possible to confirm the performance of the targets is generally performed. In the case of BRT bus, it is possible to obtain driver input and output data through vehicle CAN. The driver input data consists of the drive torque of each wheel according to the acceleration pedal position, the braking torque of each wheel according to the braking pedal position, and angle information on each wheel according to the steering angle. In addition, the output data consists of the displacement of each suspension, the speed of each wheel, and the speed of the front and rear vehicles (vehicle CAN follow the J1939 CAN protocol). However, the output data have low-resolution with the maximum sampling time of 0.1 second or above. Consequently, as in Figure 1, an environment of vehicle tests is prepared by additionally mounting RT3100, RTK on the front and rear BRT buses. RT3100 is equipped with a precise IMU sensor so that it can precisely sense vehicle motion and is equipped with a GPS sensor having an error range of 3 m so that it can precisely sense the vehicle position. Also, to supplement RT3100 position errors, RTK (GPS-based sensing devices) are installed additionally. MicroAutoBox are installed between the front and rear vehicles as CAN gateway, and all data are synchronized and logged through eDAQ.

Figure 2. *A photograph of BRT bus tests.*

After the preparation of an environment for vehicle tests, vehicle tests are conducted, as in Figure 2. As for vehicle test scenarios, three representative scenarios are chosen and implemented. Acceleration tests and deceleration tests are conducted to confirm longitudinal dynamics, and double lane change (DLC; ISO 3888-2) tests are conducted to confirm lateral dynamics. In the acceleration test, the acceleration pedal is pressed by 100% when the vehicle is stationary, and the tests are stopped when the speed reaches 80 km/h. In the deceleration test, the braking pedal is pressed by 100% while maintaining a speed of 60 km/h, and the tests are terminated when the speed reached 0 km/h (as for BRT bus, there are limitations to the acceleration pedal and the braking pedal in consideration of vehicle stability, which is restricting sudden acceleration and sudden braking). In DLC test, after a left lane change is made while maintaining a speed of 60 km/h, the tests are terminated after a right lane change is completed. The vehicle test data according to scenarios are used as reference data for the prediction model.

2.2. A General Approach to the BRT Prediction Model

Before designing a prediction model for BRT bus, it is necessary to introduce a reference paper [11] that presents a general model for articulated buses. This reference paper presents a generalized model for articulated buses where multiple vehicles can be linked and eight wheels can be applied to each vehicle. Therefore, it is necessary to explain the equations for such general vehicles, and a prediction model for BRT buses designed on MATLAB/Simulink is explained in Chapter 2.3.

In the reference paper, driver input (driving torque, braking torque, and wheel steering angles) are used, and vehicle output (longitudinal velocity u, lateral velocity v, yaw rates γ, roll angles ρ, and roll rates $\dot{\rho}$) is used. Between the input and output, there exist specific processes for additionally converting and interlocking equations. First, the front vehicle's CG point force ${F^t}_{CG}$ (longitudinal force F_x, lateral force F_y, and yaw moment M_z at CG) is calculated according to the driver input. With the calculated ${F^t}_{CG}$, the front vehicle's current state X^t (u, v, γ, ρ, $\dot{\rho}$), hitch reaction force ${F^t}_h$ (longitudinal force, lateral force, and yaw moment from the hitch), and the rear vehicle's current state X^i, the front vehicle's next state is calculated. Calculations for the rear vehicle are identical to those for the front vehicle. When they are interlocked with hitch calculation equations, a model for articulated vehicles can be developed.

$$\begin{aligned} f_{xi} &\approx Q_i / R_w \,(i=1,\cdots,8) \\ f_{yi} &= -C_{\alpha i}\alpha_i \,(i=1,\cdots,8) \end{aligned} \tag{1}$$

$$\begin{aligned} F_{xi} &= (f_{xi} + t_{xi}\Delta f_{xi})\cos\delta_i - (f_{yi} + t_{yi}\Delta f_{yi})\sin\delta_i \\ F_{xi} &= (f_{xi} + t_{xi}\Delta f_{xi})\sin\delta_i - (f_{yi} + t_{yi}\Delta f_{yi})\cos\delta_i \end{aligned} \tag{2}$$

$$F_{CG} = \begin{bmatrix} F_x & F_y & M_z \end{bmatrix}^T \tag{3}$$

where, $F_x = \sum_{i=1}^{8} t_{cxi}F_{xi}$, $F_y = \sum_{i=1}^{8} t_{cyi}F_{yi}$, $M_z = \sum_{i=1}^{8} \vec{r}_i \times F_{ci}$

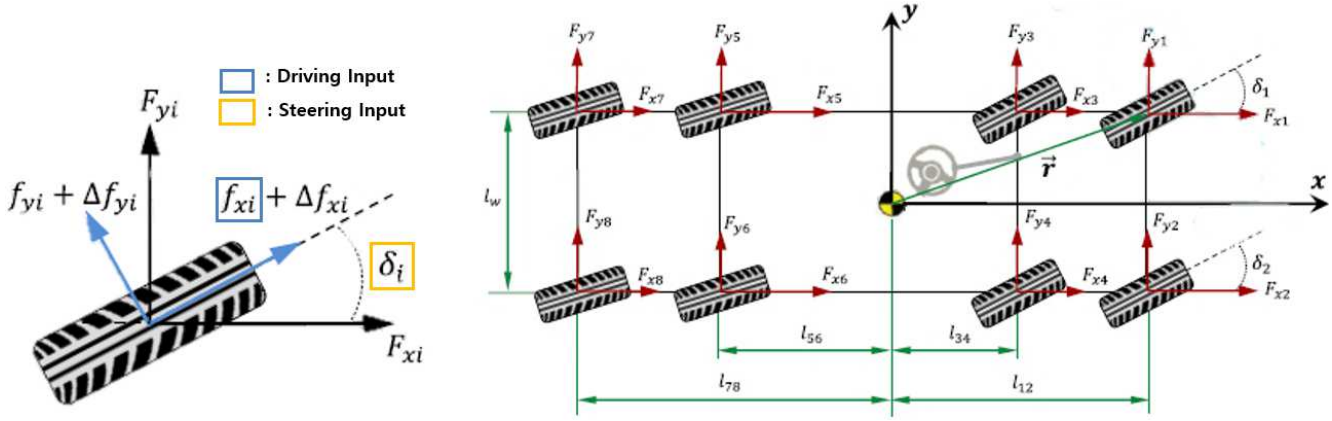

Figure 3. *Driver input and vehicle wheel model for the i-th wheel.*

Equations (1), (2), and (3) show the calculation of F_{CG} by driver input. In Equation (1), wheel torque Q_i is divided

by effective radius R_w to derive f_{xi} value (the i-th wheel's local x-axis force). In addition, cornering stiffness $C_{\alpha i}$ is multiplied by slip angle α_i to obtain f_{yi} value (the i-th wheel's local y-axis force). In Equation (2), each wheel's f_{xi} and f_{yi} and steering angle input δ_i are used to obtain F_{xi} and F_{yi} (the forces at the CG point). Because Δf_{xi} and Δf_{yi} in Equation (2) are extra forces taking general forms into consideration, they are excluded when designing a prediction model. In Equation (3), M_z (the moment at the CG point) is taken into consideration, which is calculated with $\vec{r}_i$ (the distance vector from CG point to the wheel center). In conclusion, F_{CG} can be calculated from driver input. Figure 3 shows the driver input (driving input and steering input) and position of CG point.

$$\dot{X}^t = A^t X^t + B^t F^t{}_{CG} + C^t F^t{}_h + G^t X^i \quad (4)$$

$$\dot{X}^i = A^i X^i + B^i F^i{}_{CG} + C^i F^i{}_h + G^i X^t \quad (5)$$

Equations (4) and (5) are expressing the front vehicle and the rear vehicle model in a matrix form. Superscript 't' is used for the front vehicle, and superscript 'i' is used for the rear vehicle. Because the front vehicle and the rear vehicle are organically interlocked, Equation (4) shows that $C^t F^t{}_h + G^t X^i$ (the equation related to the rear vehicle and hitch reactions) is added to $A^t X^t + B^t F^t{}_{CG}$ (the front vehicle dynamics). Detailed matrices for the front vehicle are presented in Appendix. Equation (5) is identical to Equation (4) except that superscripts 't' and 'i' are expressed conversely. In conclusion, the states of the front vehicle and the rear vehicle can be confirmed through Equations (4) and (5). Hitch force linking the front vehicle and the rear vehicle are explained in Chapter 2.3.

2.3. The Realization of the BRT Prediction Model in a Simulation Environment

This chapter presents a prediction model for BRT bus designed on MATLAB/Simulink. Firstly, application of equations presented in Chapter 2.2 in MATLAB/Simulink is explained. Then application of the vehicle specifications and tuning variables is explained.

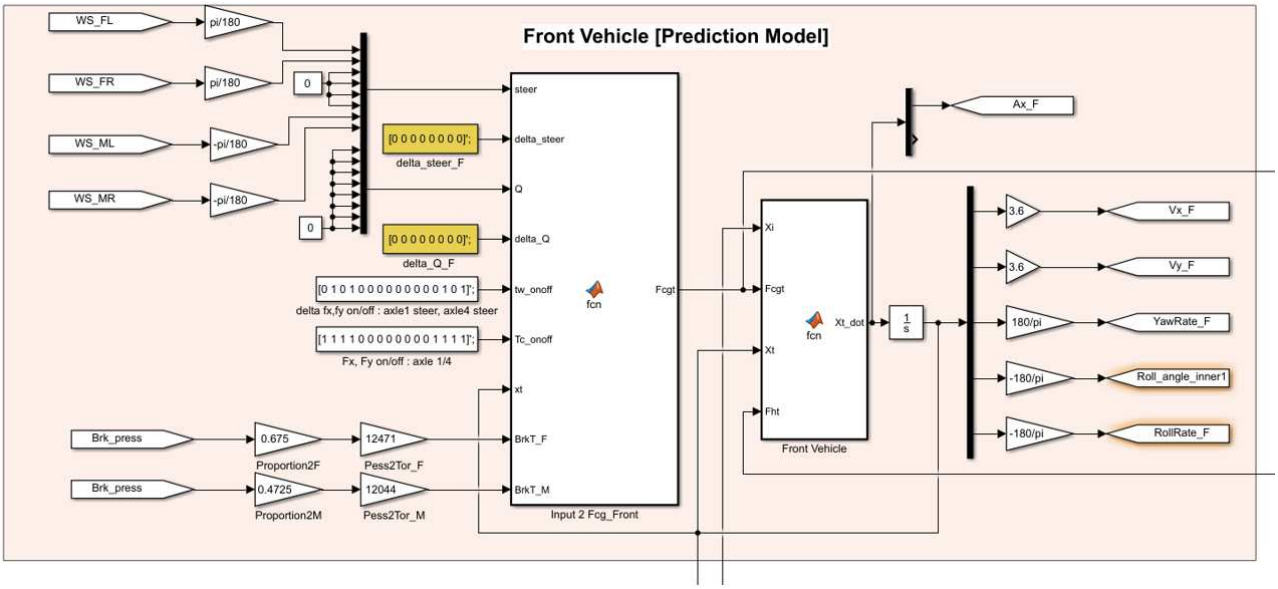

Figure 4. *The front vehicle section for the BRT prediction model.*

Figure 4 shows a Simulink model of the BRT front vehicle. An equation that converts driver input into F_{CG}, which is corresponding to Equations (1), (2), and (3), is constructed on the 'Input 2 Fcg_Front' block (the left MATLAB function block). Because driver input for the front vehicle consist only of the steering angles of the four wheel, steering values are applied only to the 1st, 2nd, 7th, and 8th wheels. Zeros are entered to the Q because driving torque does not apply to the front vehicle, and zeros are entered for 'delta_steer' and 'delta_Q' because Δf_{xi} and Δf_{yi} are extra parts.

'tw_onoff' is a switching matrix regarding whether or not to use 'delta_steer' and 'delta_Q' for the i-th wheel. Because zeros have been entered for 'delta_steer' and 'delta_Q', any value can be entered for the 'tw_onoff' matrix. 'tc_onoff' is a switching matrix regarding whether or not to use f_{xi} and f_{yi} for the i-th wheel. Therefore, ones for the 1st, 2nd, 7th, and 8th wheels are applied on in 'tc_onoff'.

'BrkT_F' and 'BrkT_M' are values that convert into braking torque applied to each axle from braking pressure generated in the master cylinder by brake pedal input. Braking torque is in a form that is entered as a negative value in driving torque input according to existing equations. However, braking torque is calculated separately because neutral gear condition and road load can be considered. With the separation, braking pedal values are converted into the master cylinder's pressure, and the pressure is distributed to

the front, middle, and rear sections at the proportional ratio of 0.675:0.4725:0.6075. Then the distributed pressure is converted into torque. As a result, the braking torque thus converted is replaced by the value for $F_x - 2BrkT_f - 2BrkT_m$ instead of F_x in Equation (3).

The vehicle dynamics equation corresponding to Equation (4) is constructed on the 'Front Vehicle' block (the right MATLAB function block). The 'Front Vehicle' block is a block where, Xi, Fcgt, Xt, and Fht are fed back and the front vehicle states are calculated. In conclusion, the units and directions of the states are adjusted through the gain block to compare with the results of BRT bus tests.

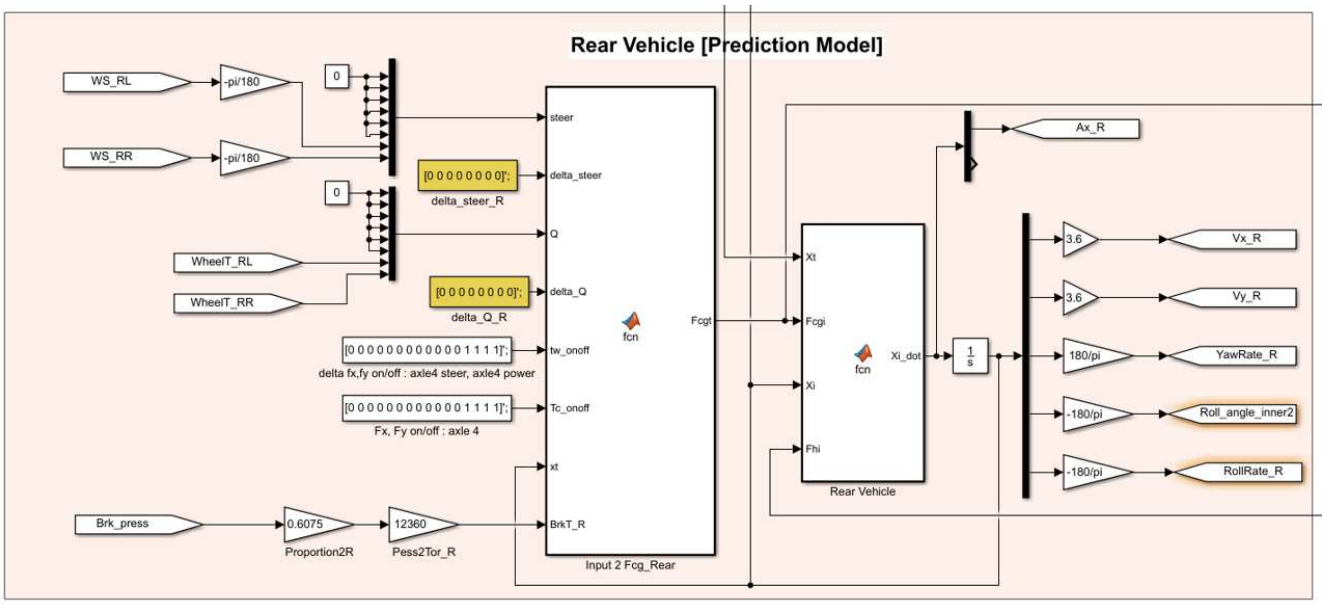

Figure 5. *The rear vehicle section for the BRT prediction model.*

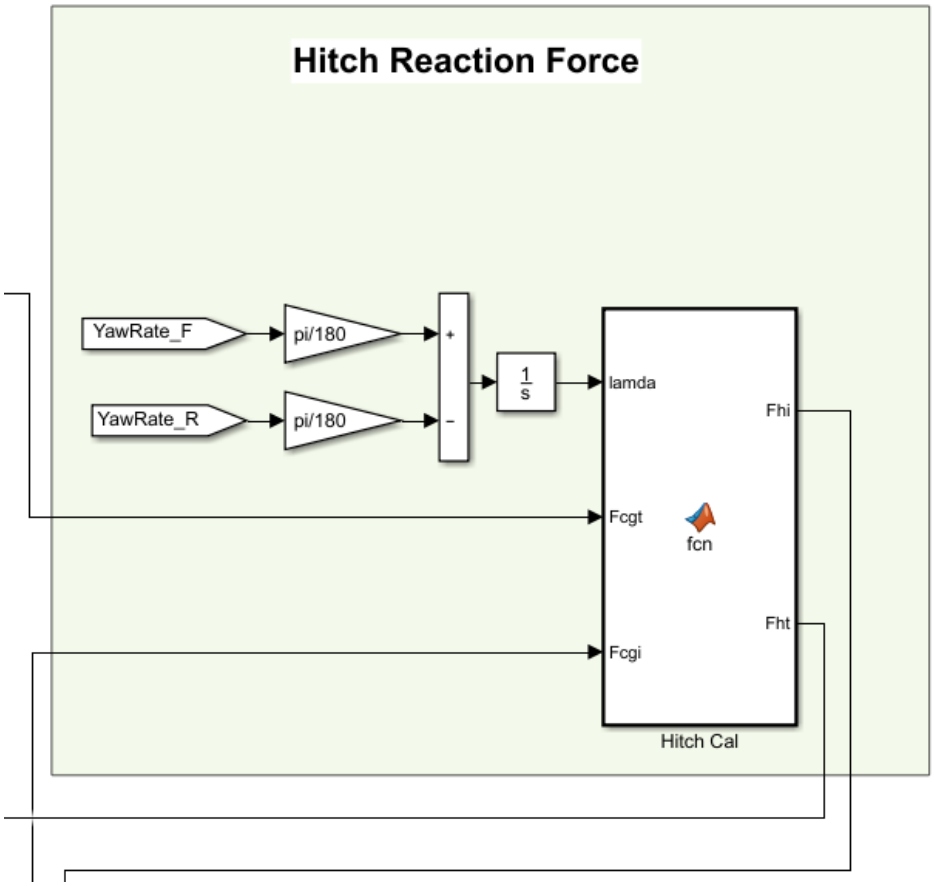

Figure 6. *The hitch section for the BRT prediction model.*

Figure 5 shows a Simulink model of the BRT rear vehicle. The construction of the 'Input 2 Fcg Rear' block and the 'Rear Vehicle' block is designed through a method identical to the design of the front vehicle. The rear vehicle differs from the front vehicle in that only two wheels used for steering angle input and driving input. Consequently, the rear vehicle is designed by defining the 7th and 8th wheels as steering angle input and driving torque input.

$$F^t{}_h = 0.5\left(\begin{bmatrix} \cos\lambda & -\sin\lambda & 0 \\ \sin\lambda & \cos\lambda & 0 \\ 0 & 0 & 0 \end{bmatrix} F^i{}_{CG} - F^t{}_{CG}\right) \quad (6)$$

$$F^i{}_h = -\begin{bmatrix} \cos\lambda & \sin\lambda & 0 \\ -\sin\lambda & \cos\lambda & 0 \\ 0 & 0 & 0 \end{bmatrix} F^t{}_h \quad (7)$$

Equations (6) and (7) are equations related to reaction from the hitches of the front vehicle and the rear vehicle. First, the reaction force to the front vehicle from the hitch can be calculated as in Equation (6). With reference coordinate of the front vehicle, the rear vehicle is rotated as much as the hitch angle. And the half of the force difference between the front F_{CG} and rear F_{CG} is defined as the hitch force transmitted to the front vehicle. The remaining half is converted into reference coordinate of the rear vehicle and defined as the hitch force transmitted to the rear vehicle. Figure 6 shows the application of Equations (6) and (7) on the Simulink block. The hitch angle is applied through the calculation of difference between yaw rates. The Fcgt (front vehicle's CG force) and Fcgi (the rear vehicle's CG force) are applied from the 'Input 2 Fcg_Front' and 'Input 2 Fcg_Rear' block. Therefore, the hitch forces (Fhi and Fht) are applied to the 'Front Vehicle' and 'Rear Vehicle' block.

Table 1. *The main parameters of BRT bus.*

Parameters	Symbol	Value	Unit
width of front, rear vehicle	$l^t{}_w$, $l^i{}_w$	2.495, 2.495	kg
Length between 1st axle to CG	$l^t{}_{12}$	3	m
Length between CG to 2nd axle	$l^t{}_{78}$	3.985	m
Length between CG to 3rd axle	$l^i{}_{78}$	3	m
Effective radius of front tire	$R^t{}_{w12}$	0.4635	m
Effective radius of middle tire	$R^t{}_{w78}$	0.5203	m
Effective radius of rear tire	$R^i{}_{w78}$	0.5212	m
Sprung mass of front, rear vehicle	$m^t{}_s$, $m^i{}_s$	13150, 13150	kg
Total mass of front, rear vehicle	m^t , m^i	28150, 27225	kg
Roll center height of front, rear vehicle	$h^t{}_r$, $h^i{}_r$	0.675, 0.621	m
Length of roll center to sprung mass CG of front, rear vehicle	$h^t{}_s$, $h^i{}_s$	1.741, 1.686	m
Distance between hitch and front, rear CG	$l^t{}_h$, $l^i{}_h$	4.9, 4.375	m
Height of hitch	h_h	0.851	m
Air density	ρ_{air}	1.225	kg/m^3
Frontal projected area	A_{air}	8.558	m^2
Drag force coefficient	C_{air}	1.06	-
Cornering stiffness of front tire	$C^t{}_{\alpha 12}$	9.368*10^6	N/rad
Cornering stiffness of middle tire	$C^t{}_{\alpha 78}$	9.368*10^6	N/rad
Cornering stiffness of rear tire	$C^i{}_{\alpha 78}$	4.684*10^6	N/rad
Yaw Inertia of front, rear vehicle	$I^t{}_{zz}$, $I^i{}_{zz}$	69992, 69992	kg-m^2
Roll Inertia of front, rear vehicle	$I^t{}_{xx}$, $I^i{}_{xx}$	8125, 8125	kg-m^2
Product of front, rear vehicle	$I^t{}_{xz}$, $I^i{}_{xz}$	0, 0	kg-m^2
Roll spring coefficient of front, rear vehicle	$K^t{}_{\varphi}$, $K^i{}_{\varphi}$	225000, 550000	N/m
Roll damping coefficient of front, rear vehicle	$C^t{}_{\varphi}$, $C^i{}_{\varphi}$	900000, 9.5*10^6	Ns/m

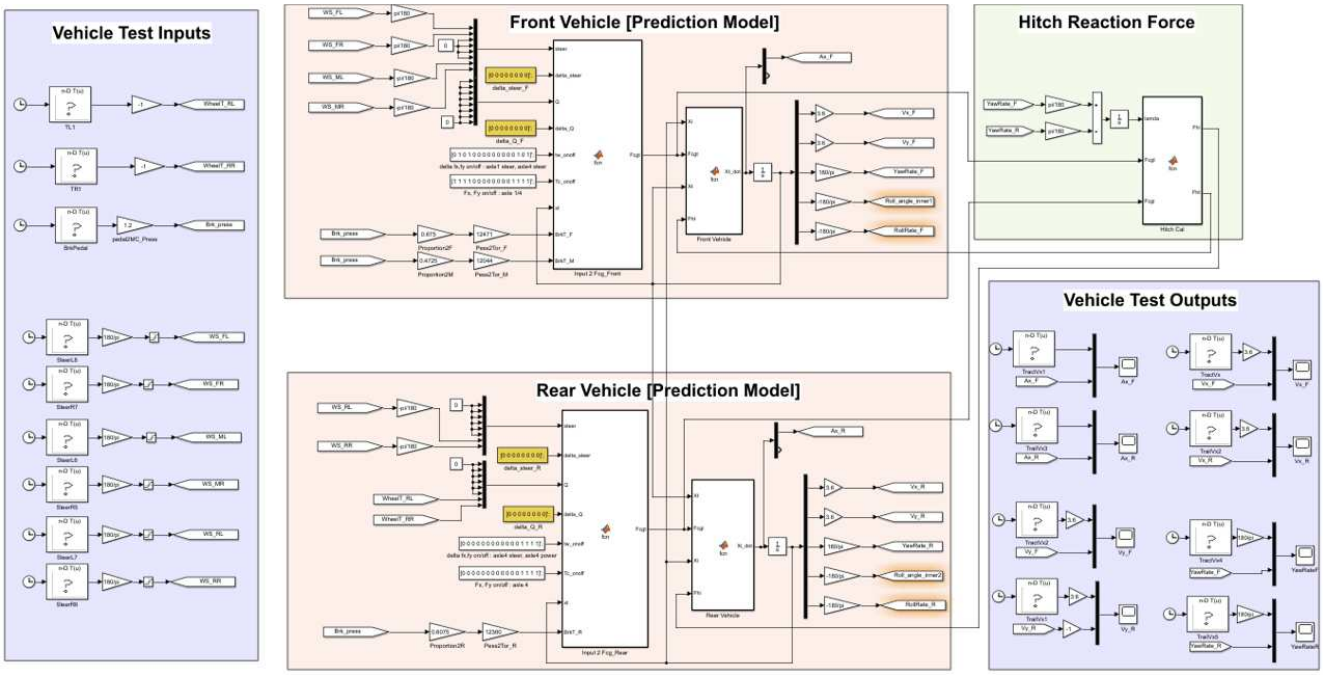

Figure 7. *A comparison environment for the BRT prediction model.*

Table 1 shows parameters that must be entered in the prediction model. In the table, known parameters, which are basic specifications such as lengths and weights, are indicated in light colors. Unknown parameters such as inertia and cornering stiffness are indicated in dark colors. In the prediction model, known parameters are entered in the model as fixed values, and unknown parameters are entered as variables. So, correlation of the prediction model can be increased by tuning the variables.

In conclusion, an environment for comparatively verifying with vehicle test results and the prediction model is constructed as in Figure 7. To construct an environment for comparative verification, the prediction model is designed on Simulink (pink-colored sections and beige-colored section). In addition, driver input logged from vehicle tests are applied to the model identically (left of sky-blue-colored section). Then output logged from vehicle tests and the prediction model's output are compared (right of sky-blue-colored section). In the sky-blue-colored sections, there are 1-D lookup table blocks. In the 1-D lookup table blocks, the vehicle test data entered, which is logged from three scenarios. Consequently, the verification results of the prediction model will be introduced in accordance with these three scenarios.

3. The Verification of the BRT Prediction Model

3.1. Correlation Results of BRT Prediction Model

The verification of the prediction model is performed by comparing the similarity between the vehicle test results and the prediction model. As for methods to compare the similarity numerically, there are: one where figures are compared simply through root mean square (RMS) errors; and one where tendencies are compared by using correlation equations [14]. In this study, correlation equation is used to compare the tendencies as a verification method of the prediction model.

When comparative verification is performed by using vehicle data, noises are observed in measured data basically. Even when identical sensors are used, different noises can be generated according to minute differences among the internal components or the connection conditions of the electric system. In other words, even when identical types of vehicles are tested in identical environments, the results yield disparate forms of noises. In vehicle modeling, such noise components should be left aside. And the similarity should be determined with a macroscopic behavior. This study therefore chooses and uses the correlation method to verify similarity among prediction models.

As for the verification scenarios for the BRT prediction model, acceleration test, deceleration test, and DLC test scenarios (three representative scenarios) are selected for verification. With acceleration and deceleration test (longitudinal tests), the Vx and Ax parameters of the front and rear vehicles are used as the verification parameters. With DLC test (lateral test), the Vy and yaw rate parameters of the front and rear vehicles are used as the verification parameters.

To verify the prediction model, the acceleration test input in the BRT bus tests is used, as in (a) in Figure 8. Because BRT buses have velocity saturation, limited driving torque is applied as the input for the prediction model. From the limited input, Vx and Ax are compared in (b) in Figure 8. As shown on the graphs, the blue curve (the result of BRT bus tests) and the red curve (the result of the prediction model) are similar. With the exception of Ax peak section, the Vx and Ax graphs are similar in the tendencies. The graphs in (c) in Figure 8 express the Vx correlation results of the front and rear vehicles. In the results, it can be confirmed that the correlation is 99% or above. The graphs in (d) in Figure 8

express the Ax correlation results of the front and rear vehicles. These results show that the correlation is 99% or above. As a result, the prediction model is developed with more than 99% correlation in acceleration test scenario.

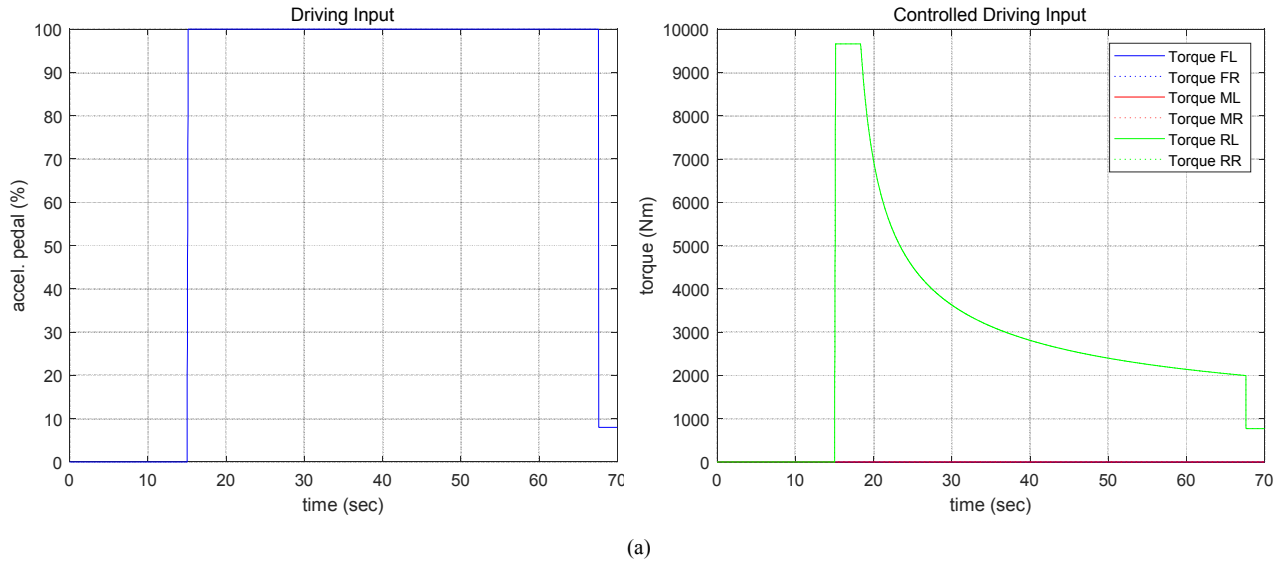

(a)

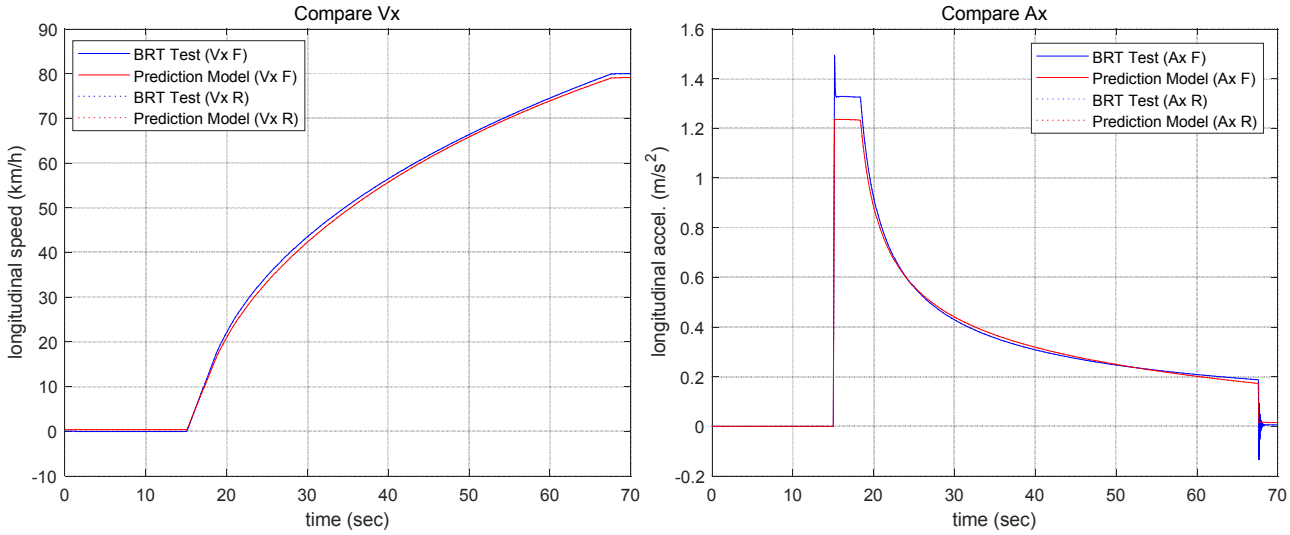

(b)

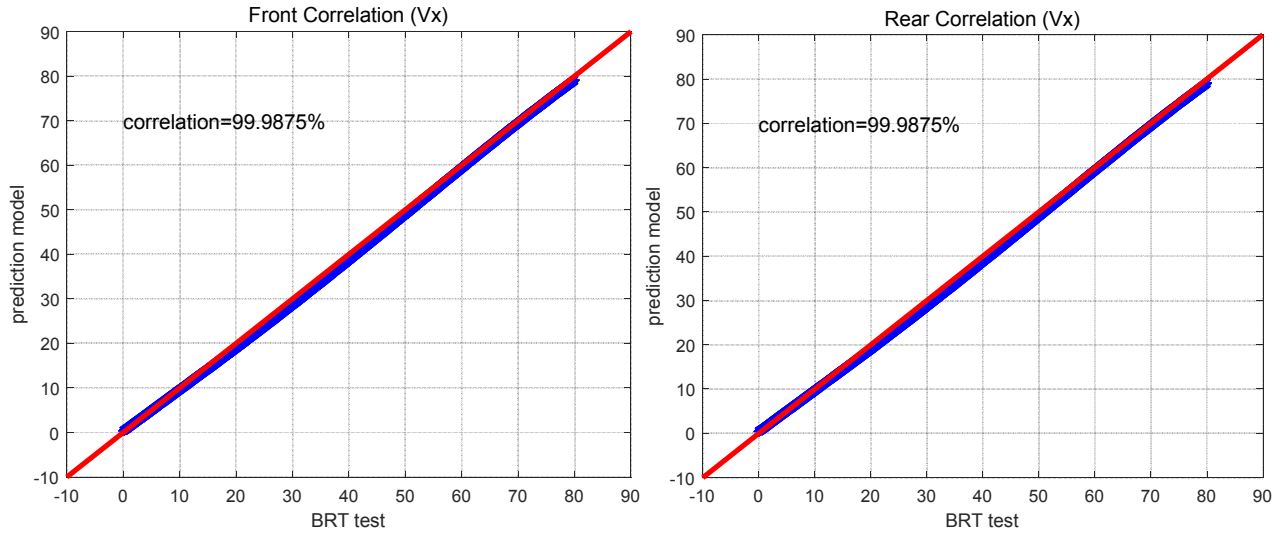

(c)

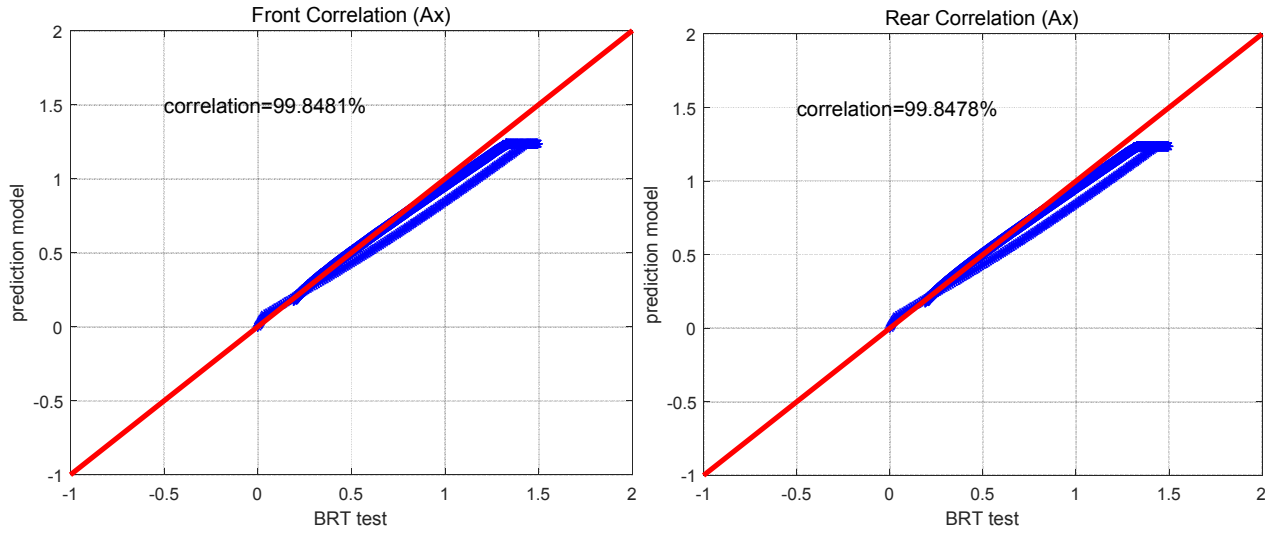

(d)

Figure 8. *The prediction model verification with acceleration test scenario.*

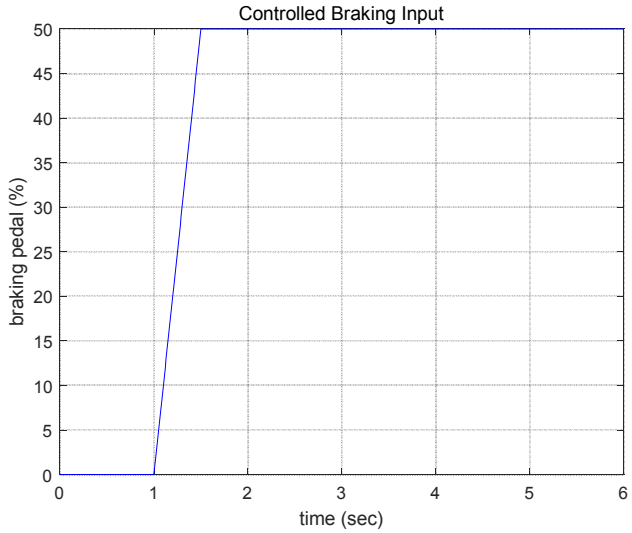

(a)

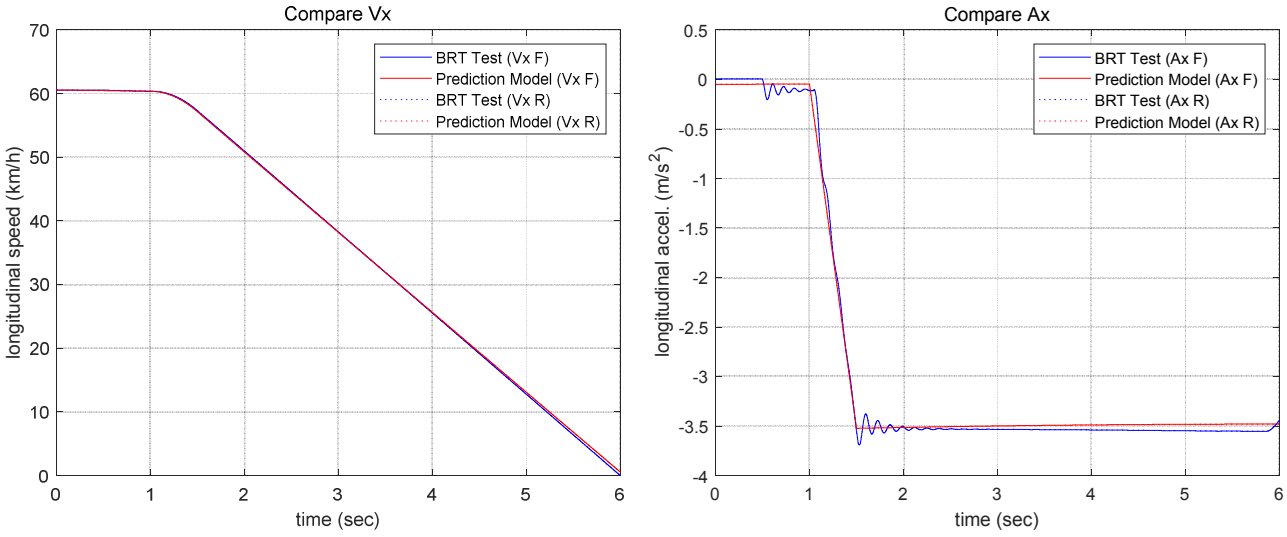

(b)

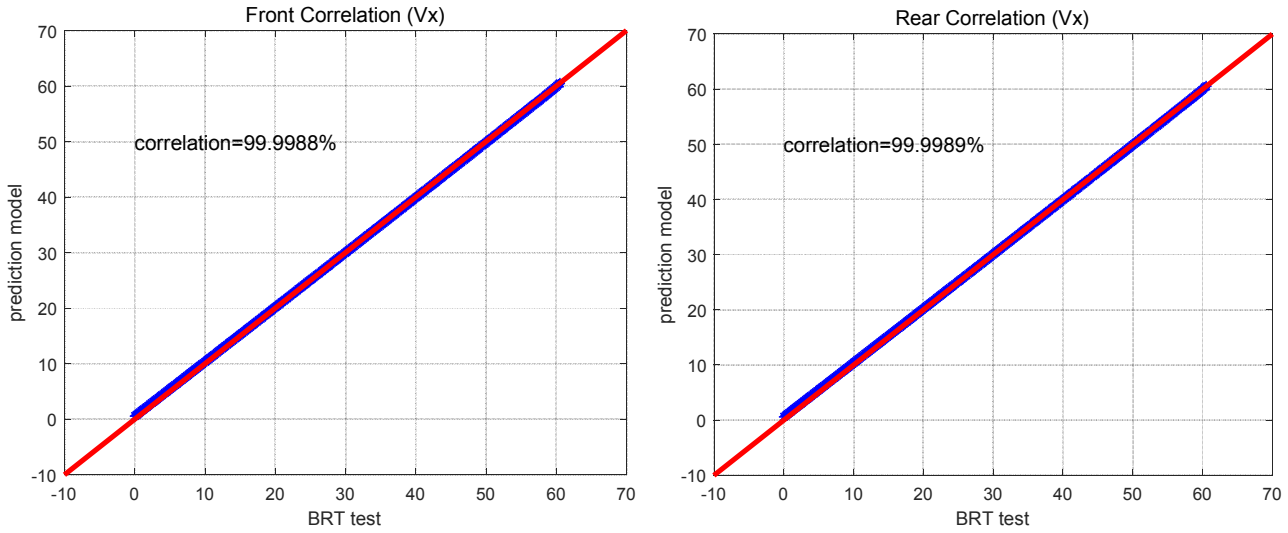

(c)

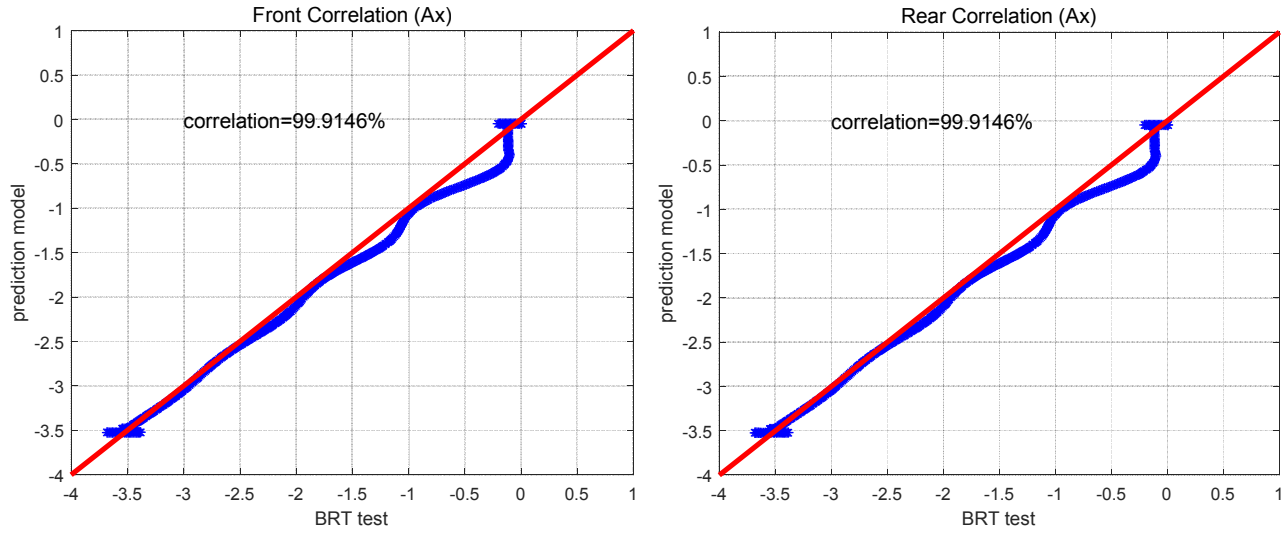

(d)

Figure 9. *The prediction model verification with deceleration test scenario.*

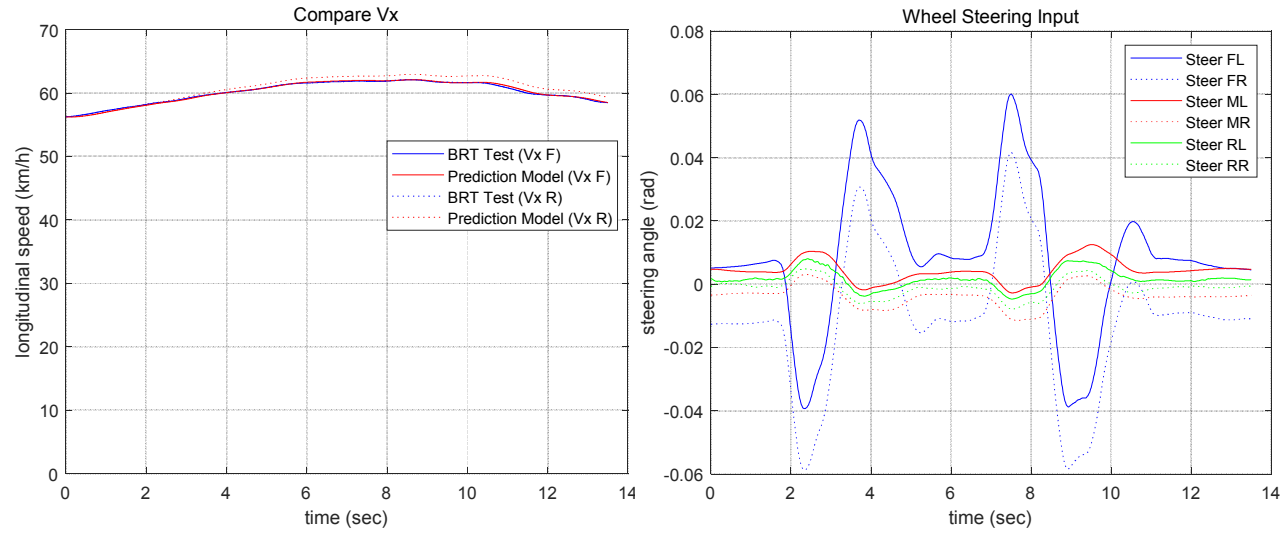

(a)

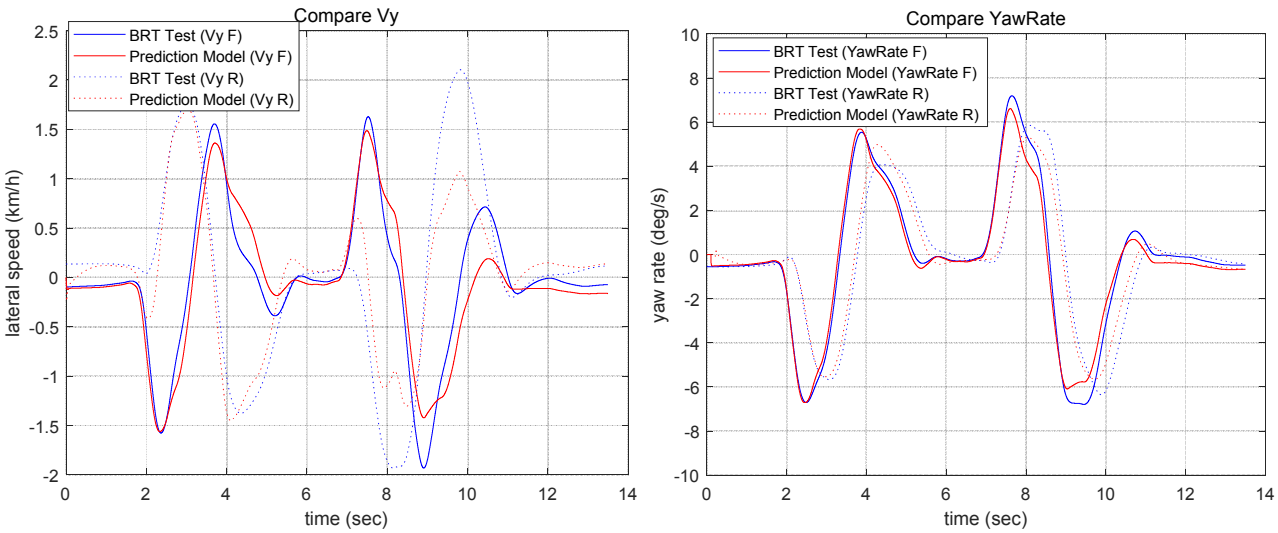

(b)

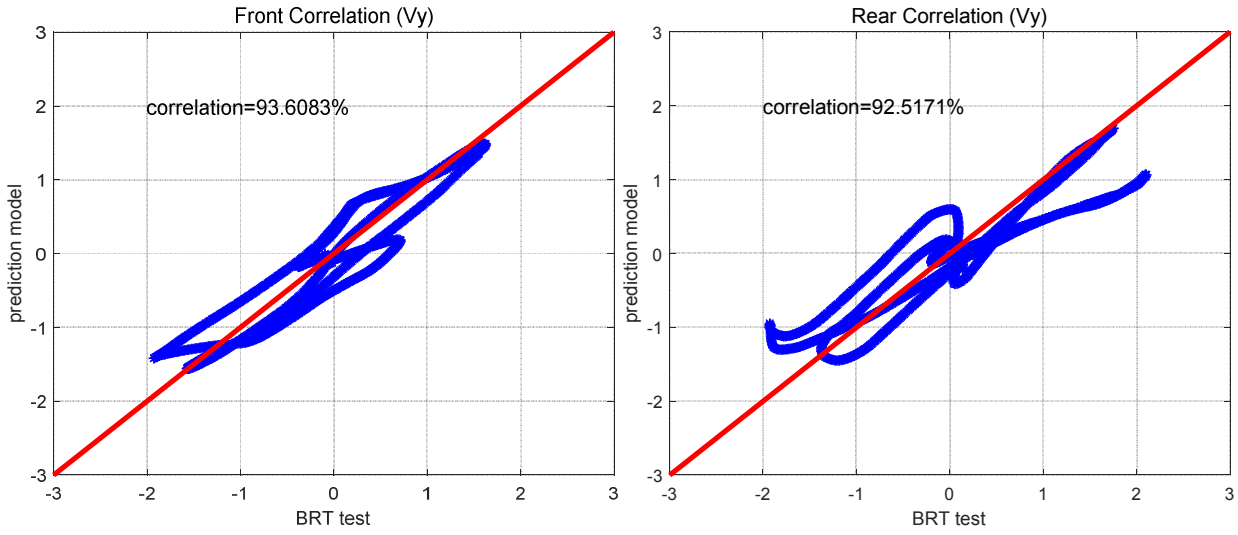

(c)

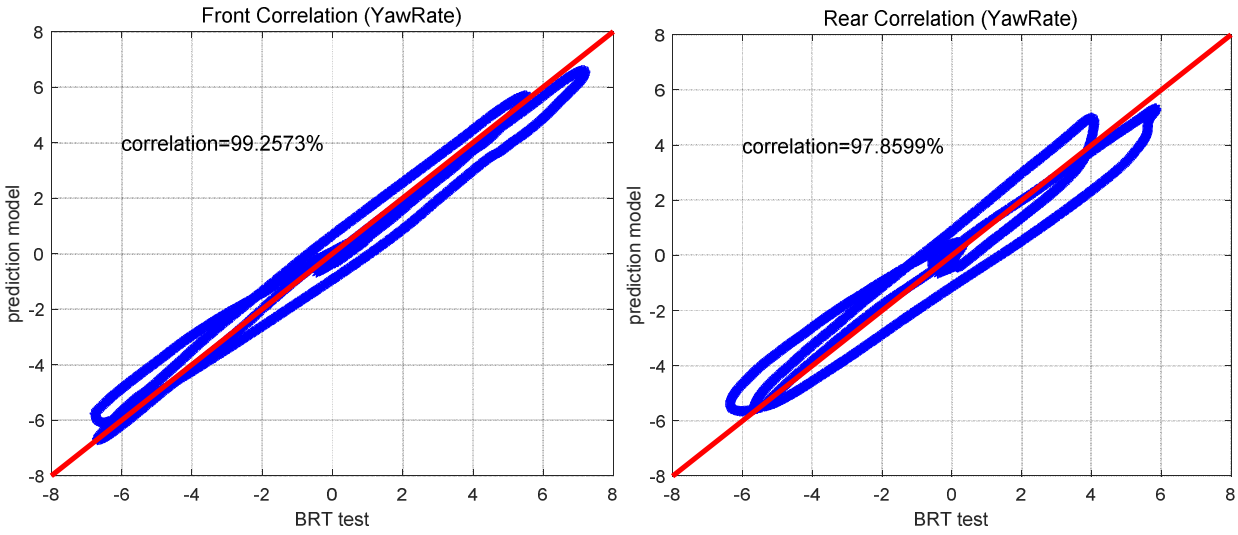

(d)

Figure 10. *The prediction model verification with DLC test scenario.*

Similarly, the deceleration test input in the BRT bus tests is used, as in (a) in Figure 9. Because BRT buses transmit braking command limited by 50% when the braking pedal amounts to 100%, limited braking input is applied as the input for the prediction model. From the limited input, Vx and Ax are compared in (b) in Figure 9. As shown on the graphs, the blue curve (the result of BRT bus tests) and the red curve (the result of the prediction model) are similar. With the exception of Ax noise sections, the Vx and Ax graphs are similar in the tendencies. The graph in (c) in Figure 9 expresses the Vx correlation results of the front and rear vehicles. In the results, it can be confirmed that the correlation is 99% or above. The graphs in (d) in Figure 9 express the Ax correlation results of the front and rear vehicles. These results show that the correlation is 99% or above. As a result, the prediction model is developed with more than 99% correlation in deceleration test scenario.

The DLC test input in the BRT bus tests is also used, as in (a) in Figure 10. The graph on the left shows Vx of a BRT bus test and the prediction model. With the high similarity of Vx, wheel steering angle inputs are applied. As for lateral input, generally the steering wheel angle input is applied. That is, the steering module dynamics must be additionally taken into consideration. However, because the purpose of this prediction model is for ADS, the consideration is unnecessary. Consequently, this prediction model is designed to control the 6 wheels directly. With the steering inputs, Vy and yaw rate are compared in (b) in Figure 10. As shown on the graphs, the differences between the blue curve (the result of BRT bus tests) and of the red curve (the result of the prediction model) are increasingly greater. Specifically, it can be confirmed that similarity of the tendencies decreases slightly. Therefore, the correlation for lateral dynamics are lower than longitudinal dynamics in (c) and (d) in Figure 10. In the graphs in (c) in Figure 10, the Vy correlation results of the front and rear vehicles show correlation 92% or above. In the graphs in (d) in Figure 10, the yaw rate correlation results of the front and rear vehicles are more than 97%. As a result, the prediction model is developed with more than 92% correlation in DLC test scenario.

Table 2. *The verification results of the BRT prediction model.*

Scenario		Front Correlation (%)	Rear Correlation (%)
Acceleration Test	Vx	99.9875	99.9875
	Ax	99.8481	99.8478
Deceleration Test	Vx	99.9988	99.9989
	Ax	99.9146	99.9146
Double Lane Change	Ay	93.6083	92.5171
	Yaw Rate	99.2573	97.8599

In conclusion, Table 2 shows the overall verification results of the prediction model. It shows the verification results according to acceleration test, deceleration test, and DLC test scenarios. In addition, representative parameters of Vx, Ax, Ay, and yaw rate are chosen in the scenarios. In conclusion, a prediction model with correlation of 92% or above has been designed.

3.2. A Prediction Model for the Development of MPC Algorithm

To design a prediction model for developing MPC algorithm, the front vehicle in Equation (4) and the rear vehicle in Equation (5) must be combined. In addition, the hitch reaction force in Equations (6) and (7) must be combined in the equations. When the combined prediction model is used, it is possible to design MPC algorithms that derive optimized control input.

$$\dot{X} = AX + BF_{CG} + CF_H + GX \tag{8}$$

where, $X = \begin{bmatrix} X^t \\ X^i \end{bmatrix}$, $A = \begin{bmatrix} A^t & 0_{5x5} \\ 0_{5x5} & A^i \end{bmatrix}$, $B = \begin{bmatrix} B^t & 0_{5x3} \\ 0_{5x3} & B^i \end{bmatrix}$,

$F_{CG} = \begin{bmatrix} F^t{}_{CG} \\ F^i{}_{CG} \end{bmatrix}$, $C = \begin{bmatrix} C^i & 0_{5x3} \\ 0_{5x3} & C^t \end{bmatrix}$, $F_H = \begin{bmatrix} F^t{}_H \\ F^i{}_H \end{bmatrix}$,

$C = \begin{bmatrix} 0_{5x3} & G^t \\ G^i & 0_{5x3} \end{bmatrix}$

Equation (8) is the combined equation of Equations (4) and (5). After the derivation of Equation (8), specific improvement is implemented as follows. First, because BRT buses have planar shape in the front, a drag force term is added to the element in Row 1 Column 1 of A^t matrix instead of 0. In addition, the value in Row 1 Column 1 of C^t matrix is changed to $1/m^t$ because of its calculation error.

$$\dot{X} = A_n X + B_n F_{CG} \tag{9}$$

$$\alpha({F_{CG}}^t - \beta {F_{CG}}^i) = {F_H}^t \tag{10}$$

$$\gamma\delta\alpha({F_{CG}}^t - \beta {F_{CG}}^i) = {F_H}^i \tag{11}$$

where, $A_n = \begin{bmatrix} A^t & G^t \\ G^i & A^i \end{bmatrix}$, $B_n = \begin{bmatrix} B^t + C^t\alpha & -C^t\alpha\beta \\ C^i\gamma\delta\alpha & B^i - C^i\gamma\delta\alpha\beta \end{bmatrix}$,

$\alpha = \begin{bmatrix} -0.5 & 0 & 0 \\ 0 & 0.5 & 0 \\ 0 & 0 & 0 \end{bmatrix}$, $\beta = \begin{bmatrix} \cos\lambda & -\sin\lambda & 0 \\ \sin\lambda & \cos\lambda & 0 \\ 0 & 0 & 0 \end{bmatrix}$, $\gamma = \begin{bmatrix} -1 & 0 & 0 \\ 0 & -1 & 0 \\ 0 & 0 & 0 \end{bmatrix}$,

$\delta = \begin{bmatrix} \cos\lambda & \sin\lambda & 0 \\ -\sin\lambda & \cos\lambda & 0 \\ 0 & 0 & 0 \end{bmatrix}$

Equation (9) is a revised prediction model created by converting Equation (8) to produce a model in the form of Ax + Bu. To turn Equation (8) into a form to Equation (9), the GX term is integrated into the AX term, and the CF_H term is integrated into the BF_{CG} term. In the integration process, AX and GX can be integrated simply. To integrate CF_H into BF_{CG}, however, it is necessary to proceed an extra process where F_H is converted into the form of F_{CG}. Consequently, as in Equations (10) and

(11), α, β, γ, and δ matrices are used to convert the hitch reaction force into the force at the CG point.

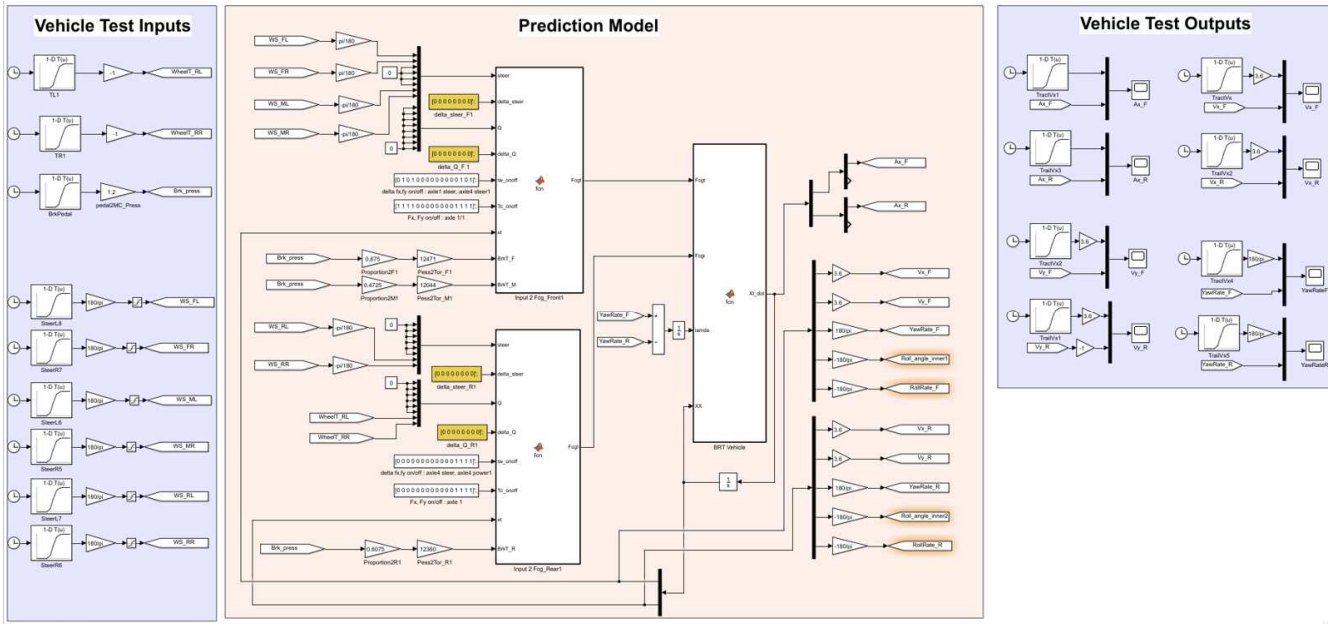

Figure 11. *The revised prediction model in Matlab/Simulink.*

In conclusion, the revised prediction model in Equation (9) is designed as in Figure 11. In the figure, it can be confirmed that driver input is converted into the front and rear vehicles' F_{CG} values and applied to the revised prediction model block. Consequently, the revised prediction model block yields the output states.

By using the revised prediction model in Equation (9), an MPC algorithm can be developed for ADS. Because this revised prediction model is derived from equations in Chapter 3.1, it is not necessary to verify the model again.

4. Conclusion

In conclusion, when a prediction model as in Equation (9) is used, an MPC algorithm can be developed for BRT autonomous driving control. The MPC algorithm makes more precise autonomous driving control possible because they implement model-based prediction control [15]. Consequently, the BRT prediction model is expected to contribute considerably to the development of the MPC algorithm.

This paper presents the development of a prediction model. As future research, this prediction model will be used to develop a real-time MPC algorithm. In order to develop the real-time MPC algorithm, it will be necessary to construct a hardware-in-the-loop system (HILS) environment where a plant model (BRT bus) can be driven in real-time. And it will be necessary to design optimization control algorithms through the prediction model. As a result, the MPC will be applied in a real BRT bus.

Acknowledgements

This research was supported by a grant (22TLRP-C152478-04) from the Transportation and Logistics Research Program funded by the Ministry of Land, Infrastructure, and Transport (MOLIT) of the Korean Government and the Korea Agency for Infrastructure Technology Advancement (KAIA).

References

[1] P. F. Muir, and C. P. Neuuman, Modeling and Control of Wheeled Mobile Robots, *Dissertation in Carnegie Mellon University*, August (1988).

[2] R. C. Coulter, Implementation of The Pure Pursuit Path Tracking Algorithm, *Technical Report CMU-RI-TR-92-01*, Robotics Institute, Carnegie Mellon University, Pittsburgh, Pennsylvania, January (1992).

[3] M. Samuel, M. Hussein, M. B. Mohamad, A Review of some Pure-Pursuit based Path Tracking Techniques for Control of Autonomous Vehicle, *International Journal of Computer Applications*, 135, 1, 0975-8887, February (2016).

[4] T. D. Gillespie, Fundamentals of Vehicle Dynamics, *Society of Automotive Engineers*, Inc. Pennsylvania, USA (1992).

[5] S. Thrun, M. Montemerio, H. Dahlkamp, et al., Stanley: The Robot that Won the DARPA Grand Challenge, *Journal of Field Robotics,* 23 (9), 661-692 (2006).

[6] M. Cibooglu, Hybrid Controller Approach for an Autonomous Ground Vehicle Path Tracking Problem, *Dissertation in Istanbul Technical University*, December, (2016).

[7] N. H. Amer, K. Hudha, H. Zamzuri, et al., Adaptive Modified Stanley Controller with Fuzzy Supervisory System for Trajectory Tracking of an Autonomous Armored Vehicle, Robotics and Autonomous Systems, 105, 94-111 (2018).

[8] S. D. Keen, and D. J. Cole, Steering Control using Model Predictive Control and Multiple Internal Models*, International Symposium on Advanced Vehicle Control*, August 20-24, (2006).

[9] H. Eric Tseng, M. Bujarbaruah, X. Zhang, F. Borrelli, Adaptive MPC for Autonomous Lane Keeping, *International Symposium on Advanced Vehicle Control (AVEC)*, December 3, (2018).

[10] R. Schmied, H. Waschl, R. Quirynen, M. Diehl, L. d. Re, Nonlinear MPC for Emission Efficient Cooperative Adaptive Cruise Control, *International Federation of Automatic Control (IFAC)*, 160-165 (2015).

[11] Y. Zhang, A. Khajepour, Y. Huang, Multi-Axle/Articulated Bus Dynamics Modeling: A Reconfigurable Approach. *International Journal of Vehicle Mechanics and Mobility,* 59, 9, 1315-1343 (2018).

[12] M. M. Michalek, B. Patkowski, T. Gawron, Modular Kinematic Modelling of Articulated Buses, *IEEE Transactions on Vehicular Technology*, vol. 69, no. 8, pp. 8381-8394 (2020).

[13] W. Wenwei, Z. Wei, Z. Hanyu, C. Wanke, Yaw Stability Control through Independent Driving Torque Control of Mid and Rear Wheels of an Articulated Bus, Institution of Mechanical Engineers, Vol. 234, no. 13, pp. 2947-2960 (2020).

[14] Gibbons, J. D., Chakreborti, S., *Nonparametric Statistical Inference*. 4th edition. Marcel Dekker, Inc. Alabama, USA (2014).

[15] L. Wang, Model Predictive Control System Design and Implementation Using MATLAB, *Advances in Industrial Control*, London, UK (2009).